Analysis of photonic crystal waveguide bends by a plane-wave transfer-matrix method

Ming Che and Zhi-Yuan Li*
Laboratory of Optical Physics, Beijing National Laboratory for Condensed Matter Physics, Institute of Physics, Chinese Academy of Sciences, P.O. Box 603, Beijing 100080, People's Republic of China
(Received 27 December 2007; revised manuscript received 28 February 2008; published 31 March 2008)

We have developed a plane-wave transfer-matrix method (PWTMM) to analyze light propagation through sharp photonic crystal bend structures. With the aid of the supercell technique, the original aperiodic waveguide bend can be modeled by a periodic scattering problem of two semi-infinite photonic crystal waveguide arrays face to face or two semi-infinite photonic crystal waveguide arrays separated by a sandwiched slab of bend region. The proposed approach has been applied to several sharp bend structures in two-dimensional photonic crystals. The calculated transmission and reflection spectra of the waveguide mode are in good agreement with existing results made by other numerical methods, even at the frequency close to the waveguide cutoff frequency. The developed PWTMM only needs to handle a single unit-cell layer domain and is therefore numerically friendly. The proposed approach can become an efficient and accurate numerical tool to understand and design high performance sharp waveguide bends in different two-dimensional and three-dimensional photonic crystals with complex geometries.

DOI: 10.1103/PhysRevB.77.125138 PACS number(s): 42.70.Qs, 78.67.−n, 41.20.Jb

I. INTRODUCTION

The efficient guiding and interconnection of light on a chip are of vital importance in telecommunication and computing applications. Conventional dielectric waveguides are restricted by radiation loss to a moderate bending radius although they can support guided modes along straight lines with high efficiency. In recent years, photonic crystals,[1–6] a class of material with a periodic distribution of dielectric function, have attracted extensive interest in the fundamental physics and potential applications to high technology. They allow one to mold the propagation of photons through photonic band gaps.[7,8] This can be explored to create future electro-optic or all-optical ultrasmall integrated optical circuits because of the peculiar propagation behavior of electromagnetic (EM) waves in defects introduced into photonic crystal (PC) structures. Some of the basic functional elements comprising the photonic crystal integrated circuit are PC waveguides, branches, and cavities.[9–15] A linear defect in a photonic crystal can create a localized mode when the frequency of a guided mode lies within the photonic band gap. The efficient confinement and propagation of EM waves through straight lines, sharp bends, and multibranches can be achieved without relying on the total internal reflection.[9] Both extensive theoretical and experimental studies have been made toward the goal of deeply and fully understanding the propagation behavior of EM waves through linear waveguides and waveguide bends created in two-dimensional (2D) photonic crystals,[9,10] 2D photonic crystal slabs,[11–14] and three-dimensional (3D) photonic crystals.[15–19]

A waveguide bend is composed of two nonparallel straight waveguides connected by a designed cross section of sharp bending structure. Because this structure does not possess periodicity along any direction, the conventional plane-wave expansion method[20,21] and transfer-matrix method[22,23] designed for a periodic photonic crystal cannot be used to understand the EM-wave propagation behavior through a waveguide bend. Instead, as the finite-difference time-domain (FDTD) method[24] is applicable to a general aperiodic structure, it is employed almost exclusively by many groups due to its simplicity in essence and simplified computational storage requirements.[9–15] However, structural boundaries such as the existence of the waveguide exits and bend present in the FDTD simulations can result in multiple reflection phenomena. Because of this, the FDTD simulation is subject to two major difficulties. First, a very large simulation domain size must be adopted in order to separate sufficiently the useful pulses and parasite multiple reflection pulses from two waveguide exits and obtain reasonable information on the transmission and reflection spectra for the bend. Without sufficient separation, the transmission and reflection pulses cannot be discerned without any ambiguity, and accurate and reliable spectrum information cannot be extracted. Second, near the waveguide cutoff frequency, there are strong fluctuations in the transmission and reflection spectra calculated by the FDTD technique. As high as 120% transmissivity can be found at some definite frequencies.[9,15] This oscillation is mainly ascribed to the widening of the long-wavelength component during the propagation process of pulses along the waveguide. This widening results in overlaps among the useful and the parasite pulses. Therefore, strong oscillation occurs when one tries to separate these pulses. To solve these problems in the usual FDTD simulations, sophisticated absorbing boundary conditions[25,26] have been deliberately designed to reduce spurious reflected pulses. This approach has to ensure that the perfectly matched layers perform equally well for all incidence directions and all k wave numbers included in the wave packet. Recently, other frequency-domain theoretical approaches beyond the FDTD technique have been developed in literatures to calculate the propagation of EM waves through sharp bends of photonic crystal waveguides. These include the eigenmode examination method,[27] the Wannier-basis field expansion method,[28,29] the multiple multipole method,[30,31] and the finite-element method.[32,33] These methods can overcome the numerical difficulties encountered in a usual FDTD simulation.

In this work, we propose a approach that is physically simpler, numerically friendly, and quantitatively accurate to investigate EM wave propagation through sharp photonic crystal waveguide bends and the corresponding spectrum information. Our method is based on the plane-wave transfer-matrix method (PWTMM) that has recently been extensively utilized to study EM wave scattering at general photonic crystal interfaces.[34–39] The method can handle both 2D PC structures (at both TM and TE polarization modes) and 3D PC structures.[34–36] In addition to the routine solution of band structures for an infinite photonic crystal and transmission spectrum for a finite-length slab of photonic crystal, this method has been developed to allow a solution of the wave scattering problems of semi-infinite PC structures without any difficulty of multiple reflection at the PC interfaces.[37–39] It has been well known that such difficulty usually exists in FDTD simulations and can only be removed with great caution by deliberately designed absorbing boundary conditions.[25,26]

This paper is arranged as follows. In Sec. II, we discuss how to adopt the basic idea of PWTMM to handle the wave propagation through aperiodic PC waveguide bends. In Secs. III and IV, we take several examples of 2D PC waveguide bend structures to address the efficiency of the proposed method. In Sec. IV, we further discuss how to construct an optimal supercell model to reduce the numerical computation burden of PWTMM in application to a general PC waveguide bend. In Sec. VI, we summarize this paper.

II. EXTENSION OF PLANE-WAVE TRANSFER-MATRIX METHOD TO PHOTONIC CRYSTAL WAVEGUIDE BENDS

As we have discussed in Sec. I, there exist two major difficulties that obstruct accurate FDTD simulations of PC waveguide bends. One is the multiple reflection at the waveguide exits, the other is the overlap between the incident and reflection pulses, and overlap between the transmission and parasite reflection pulses from the exits. In other frequency-domain methods, the major difficulty is to extract the coefficient of the reflection and transmission mode from the total field distribution. The best way out of these difficulties is to consider two infinitely-long waveguides connected through the sharp waveguide bend because no multiple reflection due to the waveguide exits will be present in such model structures.[37–42] Recent studies show that PWTMM can be an ideal numerical tool for this task because this method can handle intrinsic eigenmode scattering at any complex structure composed of two semi-infinite PC structures and related PC waveguide structures when the usual supercell technique is incorporated.[37–39]

The basic point of PWTMM is that any EM field can be represented by plane-wave functions that are associated with a particular periodic lattice. In this aspect, it seems that the current PC waveguide bend structure cannot be handled by PWTMM due to the lack of periodicity in the waveguide bend along any direction. However, when we consider that the sharp waveguide bends are formed by two semi-infinite PC waveguides face to face or by two semi-infinite PC waveguides connected through a general slab structure (bend section), things become different. The originally aperiodic bend structure can now be incorporated with the usual supercell technique and then modeled by wave scattering problem in periodic structures. As a result, it turns out that PWTMM is applicable in solving the wave scattering problem of the aperiodic PC waveguide bend structure.

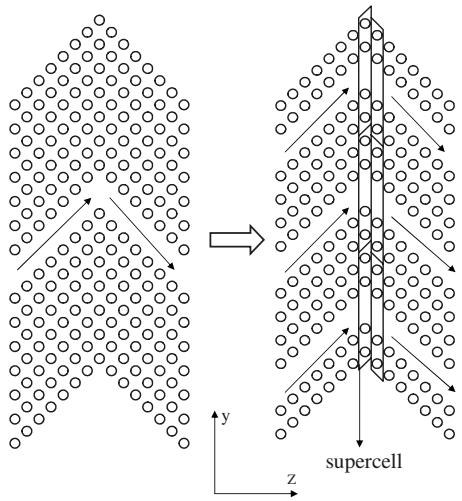

FIG. 1. Schematic diagram of the supercell technique used to handle the EM-wave propagation behavior through a 2D PC waveguide bend. The original aperioidc waveguide sharp bend problem is converted into a periodic waveguide array scattering problem. The photonic crystal is periodic in the YOZ cross-section plane and homogeneous along the x axis.

To see how this can be possible, we take as an example and look at a 2D PC waveguide bend structure built in a square lattice of dielectric rod embedded in the air background. As schematically depicted in Fig. 1(a), the structure is a 90° sharp bend composed of two straight waveguides. Because only waveguide modes localized around the waveguide central axis are considered, we can introduce other artificial waveguides that are parallel to the original input and output waveguides. The situation is depicted in Fig. 1(b). Note that the 2D photonic crystal is periodic in the *YOZ* plane and homogeneous along the x axis. The stacking direction of the cylinder is along the z axis (along the ΓM direction of the square lattice). In this direction, each layer behaves like a one-dimensional (1D) diffraction grating that is perfectly periodic along the y axis. The 1D grating has a period of $\sqrt{2}a$, with the primitive lattice vector being $\vec{a}_2=(\sqrt{2},0)a$, where a is the lattice constant of the crystal. Another primitive lattice vector along the z-axis direction is $\vec{a}_3=(\frac{\sqrt{2}}{2},\pm\frac{\sqrt{2}}{2})a$ for the left-side and right-side photonic crystals, respectively. For more details on how to use PWTMM to solve the band structures and transmission spectrum for this 2D photonic crystal, the readers are referred to Refs. 34 and 35. A supercell depicted in Fig. 1(b) consisting of up to m unit cells centered at the axis of the waveguide has been adopted. The primitive lattice vector of this supercell is $\vec{a}_2=(\sqrt{2}m,0)a$ and $\vec{a}_3=(\frac{\sqrt{2}}{2},\pm\frac{\sqrt{2}}{2})a$ for the left-side and right-side waveguide arrays, respectively. When the distance between two adjacent parallel auxiliary waveguides, which is

$\sqrt{2}ma$, is large enough so that leakage of EM waves from one waveguide to the other is negligible, the existence of all the auxiliary waveguides do not bring any impact to the original wave propagation problem in regard to the transmission and reflection of waveguide modes at the sharp bend. If the parallel waveguides have equal lateral spacing, then the whole structure is simply composed of two semi-infinite periodic waveguide arrays face to face and in touch with each other or two semi-infinite periodic waveguide arrays connected through a slab of the sharp bend array. Now, it becomes clear that the original aperiodic bend structure has been modeled by a periodic structure of sharp bend supercell, to which all the theoretical formulation and numerical techniques of PWTMM can be readily applied.

The first practical systems we investigate are waveguide bend structures created in a 2D photonic crystal consisting of a square lattice of dielectric cylinders in air. To make a good reference to existing results in the literatures, we take exactly the same parameters as those reported in Ref. 9, The refractive index of the rod is 3.4, corresponding to GaAs at the canonical wavelength of 1.55 μm, and the radius of the cylinder is $r=0.18a$, where a is the lattice constant of the crystal. There is a wide fundamental photonic band gap between the first and second bands for a perfect lattice under TM polarization (where the electric field is parallel to the cylinder axis). A waveguide can be generated by simply removing one row of cylinders in an otherwise perfect lattice, which is called a W1 waveguide. This waveguide supports a single-mode waveguide state within the band gap. The geometrical configurations of the two different waveguide bend structures that we study in this work are schematically displayed in Figs. 2(a) and 2(b). Here, the coordinate of the system is set in accordance with the PWTMM, where the stacking direction of the PC unit-cell layer (from left to right) is set to be the z axis, which is just the (11) direction of the square lattice, and the lateral periodic direction is set to be the y axis. The two 90° bend structures are formed by connecting a (10) direction straight waveguide (along the ΓX direction of the square lattice) and a (01) direction straight waveguide (along another ΓX direction). The only difference between these two structures is the position of a single cylinder lying right at the corner of the bend region. The bend in Fig. 2(b) can be assumed to have zero radius of curvature. The propagation behavior of these two bend structures has been studied in detail in Ref. 9 by means of the FDTD technique and, later, by other frequency-domain methods.[25–33]

We can now apply the PWTMM to solve the wave scattering problem of the sharp bend structures. Because semi-infinite PC waveguide array structures are considered, the intrinsic transmission and reflection coefficients of an input waveguide mode at the sharp bend can be calculated following the basic procedures that have been described in detail in Ref. 35. The major processes are basically as follows. First, we denote the left and right semi-infinite PC waveguide array structures as PC1 and PC2, respectively. Second, we solve the eigenmodes (including eigenvalues and eigenvectors) of the two supercell photonic crystals in the plane-wave space and write the EM fields in the form of eigenmode superposition. Note that the eigenmodes are associated with the unit-cell transfer matrix and involve both propagation

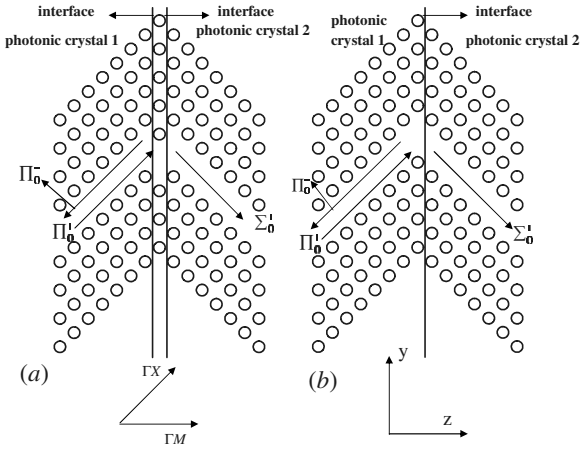

FIG. 2. Geometrical configuration of two different 90° waveguide bend structures introduced into a square lattice of dielectric cylinders in air. Each waveguide is created by removing a single row of cylinders in an otherwise perfect lattice. The cylinder has a refractive index of 3.4 and a radius of $r=0.18a$. These two structures are modeled by two semi-infinite photonic crystal waveguide arrays (photonic crystal 1 and photonic crystal 2) face to face in touch (b) or by two semi-infinite photonic crystal waveguide arrays (photonic crystal 1 and photonic crystal 2) connected through the central sandwiched slab (a). The eigenmode scattering problem can be solved to yield the transmission waveguide mode Σ_0^+ and the reflection waveguide mode Π_0^- under an input waveguide mode Π_0^+.

and nonpropagation modes. Physically, one of these eigenmodes must be the waveguide mode of the straight PC waveguide. Third, we match the boundary conditions of EM fields at the boundary of the two PCs, which might directly touch each other face to face or be separated by the central sandwiched slab. From this, we can find the relation between the transmission eigenmode coefficients (in PC2), the reflection eigenmode coefficients (in PC1), and the incident eigenmode coefficient (in PC1). Fourth, we solve the linear simultaneous equations and find all the unknown eigenmode coefficients. From this, we can straightforwardly calculate the transmission and reflection coefficients of an incident eigenmode (the waveguide mode) due to the sharp bend. If the PCs have multiple propagation eigenmodes that carry energy fluxes, then we encounter a multimode structure problem. The scattering coefficient of an incident eigenmode into a particular eigenmode (either reflection eigenmode in PC1 or transmission eigenmode in PC2) can also be directly obtained from the PWTMM calculation.[36]

Although the general procedures of a theoretical analysis are similar to those in Ref. 35, things are slightly different now. In Ref. 35, only normal incidence problems are discussed. In this case, the parallel Bloch-wave vector k_y (which is a conservative quantity and an input parameter in the PWTMM calculation) is exactly zero. It is then very convenient to find all the eigenmodes (represented by the perpendicular wave vector k_z) corresponding to a given frequency ω following the general procedure of PWTMM.[34] In the current sharp waveguide bend structure, the incident waveguide mode, which should be the eigenmode of PC1, propagates along the waveguide in a direction that is 45° inclined with the stacking direction of the PC unit-cell layers. Let us de-

note the incident Bloch-wave eigenmode (the waveguide mode) as Π_0^+, which is characterized by parameters (ω, k_y, k_z). When this mode obliquely impinges on the interface between the semi-infinite photonic crystal PC1 (left) and the semi-infinite photonic crystal PC2 (right), one part of energy power is reflected back and evolves into another Bloch-wave Π_0^- (the reflection waveguide mode) and the other part of energy power transmits through the interface and evolves into a Bloch-wave Σ_0^+ in PC2 (the transmission waveguide mode).

To employ the PWTMM for a solution of the transmission and reflection spectra of the sharp bend, we need to first determine all the eigenmodes of the waveguide arrays (PC1 and PC2) accurately and pick up from these eigenmodes the single propagation mode that corresponds to the waveguide mode of the original W1 PC waveguide under the oblique incidence situation. To achieve this goal, we first accurately compute the eigenmodes of the guided modes in the straight waveguides by means of the PWTMM in combination with the supercell technique. As we have mentioned above, in the PWTMM solution to the eigenmodes in the first Brillouin zone of a photonic crystal, the eigenfrequency ω and the lateral Bloch-wave vector k_y are explicitly given as input parameters and k_z is left to be determined from the unit-cell transfer matrix. The PWTMM is most numerically economical to compute the photonic band structure parallel to the layer stacking direction ($\theta=0°$).[37] However, the Bloch-wave Π_0^+ [with $\vec{k}=(k_y,k_z)$] under the current problem of the 90° sharp waveguide bend lies at an oblique angle of $\theta=45°$ with respect to the stacking direction. We have to project the Bloch-wave vector onto the layer stacking direction ($\theta=0°$) and obtain the lateral Bloch-wave vector in this direction, which is k_y. Then, we calculate the dispersion along the layer stacking direction of the photonic crystal and find out the eigenmodes in the neighboring region of k_z, which are denoted as (k'_{zi}, ω_i) $(i=1,2,\ldots,n)$ for a series of frequency points ω. Matching k'_{zi} to the prefixed value of k_z (which is equal to k_y in the current problem) through the interpolation technique, we can pick up the exact value of eigenfrequency ω that corresponds to the Bloch-wave Π_0^+, namely, an eigenmode propagating along the original waveguide direction. We have checked the band structure of the waveguide as well as the eigenmode field profile and energy flux of the waveguide mode by the above numerical technique by comparing them to the PWTMM calculation results for the same straight waveguide under a normal incidence situation where k_y is zero, which can be very precise without any troublesome interpolation technique. A very excellent agreement has been found, which verifies the efficiency and accuracy of the projection and interpolation method.

Now that we have obtained the exact waveguide mode solution of (ω, k_y, k_z), we take them as input parameters and calculate all the eigenmodes of PC1 and PC2 under the given oblique angle. With these eigenmodes at hand, we directly follow the procedures of the PWTMM and calculate the coefficient of the reflection waveguide mode in PC1 and the transmission waveguide mode in PC2 by considering Bloch-wave eigenmode scattering at the interface of two semi-infinite PC structures in touch face to face or by considering Bloch-wave eigenmode scattering at the interfaces of two semi-infinite PC structures connected with a general slab sandwiched between them.[37] The intrinsic transmission and reflection spectra of the input waveguide mode by the sharp bend structure can be directly obtained. At this step, the wave propagation problem of sharp bend structures has been completely solved. Looking back again at the above numerical procedures to attack the difficult problem by means of PWTMM, we find that the major numerical obstacle lies at the determination of the exact eigenmode corresponding to the incident waveguide mode. This step spends a large fraction of computation time. Any improvement to this step by finding more efficient numerical techniques to solve the desired waveguide mode should greatly help make the PWTMM more numerically friendly.

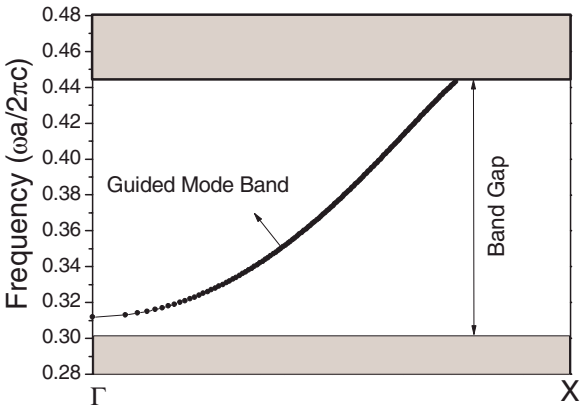

FIG. 3. (Color online) Plot of the calculated band structure of the guided modes in the waveguides shown in Fig. 3 by means of PWTMM. The gray regions represent the lower and upper band edges of the photonic band gap for the background bulk material of photonic crystals.

III. SHARP WAVEGUIDE BENDS IN SQUARE LATTICE STRUCTURES

Our first example are the bend structures shown in Fig. 2. The 2D square lattice 90° sharp bend structures have somewhat become a standard problem that any new approach needs to first consider in order to demonstrate its power and efficiency since the first study made in Ref. 9. The calculated band diagram of the guided mode by means of the PWTMM is plotted in Fig. 3. A supercell consisting of up to 11 unit cells centered at the axis of the waveguide has been adopted, and the distance between the adjacent waveguide axes is $11\sqrt{2}a$ in the y-axis direction of Fig. 1. Up to 169 plane waves have been used to calculate the dispersion of the guided mode. The numerical accuracy is better than 0.5%. The fundamental TM band gap lies between frequencies $0.302(2\pi c/a)$ and $0.443(2\pi c/a)$, where c is the light speed in vacuum. The gray regions represent the upper and lower edges of the photonic band gap, and they are occupied by continuum photonic bands for the background bulk material. Each straight waveguide in Fig. 2 supports single-mode operation of guided waves extending from a frequency of $\omega=0.312(2\pi c/a)$ at the wave vector $k=0$ to the upper band

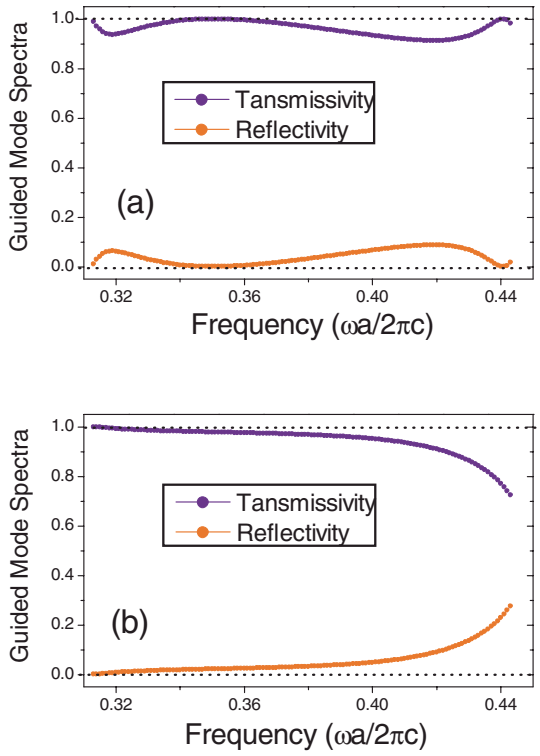

FIG. 4. (Color online) Calculated transmissivity and reflectivity spectra for (a) the waveguide bend structure shown in Figs. 2(a) and 2(b) the waveguide bend structure shown in Fig. 2(b).

edge at about $k=0.76(\pi/a)$. To check the accuracy of the PWTMM calculations, we have also calculated the dispersion of the guided mode in this structure using the standard plane-wave expansion method in combination with the supercell technique.[20,21] A supercell consisting of 11×1 cylinders and up to 2300 plane waves have been used in the calculation. A TM band gap extends from frequency $0.302(2\pi c/a)$ to $0.443(2\pi c/a)$. The overall dispersion of the guided mode excellently coincides with that displayed in Fig. 3.

Following the above procedure to calculate the transmissivity and reflectivity of the PC waveguide bends, we have systematically investigated the guided mode spectra for the waveguide bend structure. Figures 4(a) and 4(b) display the calculation results of the spectra for the two bend structures shown in Figs. 2(a) (called bend 1 structure) and 2(b) (called bend 2 structure), respectively. The two structures have the same configuration except that the single cylinder at the corner is in a different position. The calculations are performed on an AMD 2.2 GHz Opteron processor CPU. The computational memory required is at a relative small value as 120 Mbytes, and the calculation time for each frequency point in the spectrum is about 3 min. Several major features can be seen from Figs. 4(a) and 4(b). First, for bend 1 structure, the bending efficiency is over 90% in the entire range of the guided mode band. In the range between $\omega=0.338(2\pi c/a)$ and $\omega=0.362(2\pi c/a)$ or, correspondingly, between $k=0.325(\pi/a)$ and $k=0.450(\pi/a)$, there appears a high-transmissivity (above 99%) and low-reflectivity (below 1%) plateau. Second, for the bend 2 structure, the transmissivity (reflectivity) almost decreases (increases) monotonically with respect to the frequency. As small as below 1% reflectivity can be found at low frequencies close to the waveguide cutoff frequency. However, nearly 30% reflectivity can occur for those guided modes close to the upper band edge. Finally, the transmissivity and reflectivity sum up to exactly unity as required by total energy flux conservation in the entire range of the guided mode band. The overall variation profiles of the transmission and reflection spectra are in good accordance with other later simulations by means of theoretical approaches and models either in the time domain or in the frequency domain,[25–33] as one can find by comparing Figs. 4(a) and 4(b) in the current work with Fig. 9 in Ref. 30 (the multiple multipole method), Fig. 1 in Ref. 29 (the Wannier-basis field expansion method), Figs. 2(a) and 2(b) in Ref. 33 (the finite-element method), and Figs. 10 and 11 in Ref. 27 (the eigenmode examination method). For example, at $\omega=0.347(2\pi c/a)$, we find the transmissivity $T=99.4\%$ and the reflectivity $R=0.06\%$ for the bend 1 structure and the transmissivity $T=97.9\%$ and the reflectivity $R=2.1\%$ for the bend 2 structure. In the eigenmode examination method, we find the transmissivity $T=99.4\%$ and the reflectivity $R=0.05\%$ for the bend 1 structure and the transmissivity $T=97.9\%$ and the reflectivity $R=2.1\%$ for the bend 2 structure.[27] The excellent agreement between different methods is obvious. On the other hand, the numerical difficulties encountered in the original FDTD simulations have been overcome completely. The strong fluctuations in the transmission and reflection spectra calculated by the FDTD technique near the waveguide cutoff frequency (see Fig. 2 in Ref. 9) no longer exist here. The reason is that the incident wave, transmission wave, and reflection wave within each waveguide can now be discriminated very accurately in the frequency domain by the PWTMM.

Our current PWTMM has several advantages. First, semi-infinite PC waveguides are considered in the simulation. Intrinsically, no waveguide exits in the input and output pore exist; therefore, no reflection occurs at the exits. In comparison, very careful and troublesome absorbing boundary conditions must be used in modified FDTD simulations.[25,26] Second, in our PWTMM, it is enough to only consider one single unit-cell layer in eigenmode solutions for the entire waveguide band. In comparison, in the modified FDTD simulation, a sufficiently large simulation domain is still required to separate the input pulse and the reflection pulse in the input domain in order to have a sufficiently fine resolution of reflection spectrum. This is especially true for spectrum close to the waveguide cutoff frequency where strong dispersion occurs. Third, the PWTMM automatically picks up the coefficients of transmission and reflection waveguide modes.

To further demonstrate the effectiveness and accuracy of the proposed approach, we vary the length of the (10) waveguide section (along the ΓM direction), giving the lengths $L=0.5\sqrt{2}a$, $L=1.5\sqrt{2}a$, and $L=2.5\sqrt{2}a$. The corresponding configuration of the waveguide bend structures is depicted in Figs. 5(a) (bend 1 structure), 5(b) (bend 3 structure), and 5(c) (bend 4 structure). Note that these structures are in exact correspondence to the structures studied in Fig. 4 of Ref. 9. Figure 6 displays the calculation results of the reflection

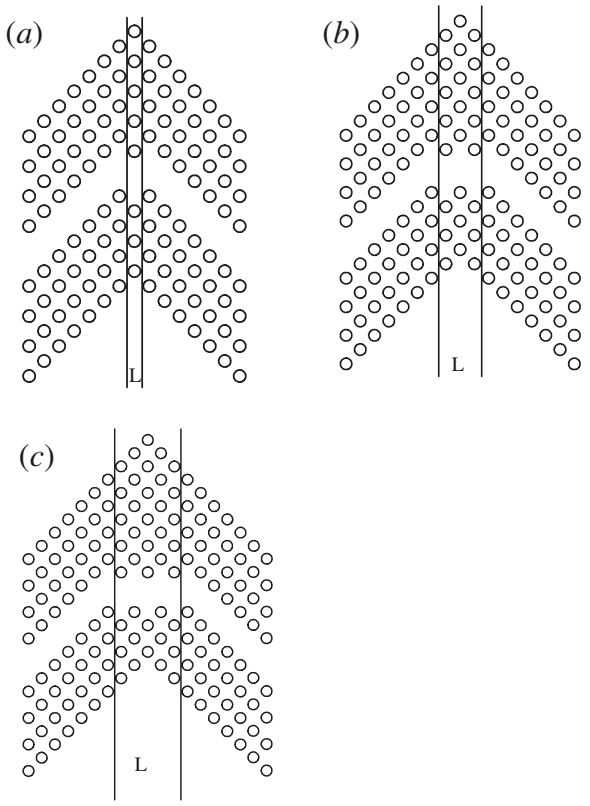

FIG. 5. Three different geometries of the 90° waveguide bend structure introduced into a square lattice of dielectric cylinders in air. The cylinder has a refractive index of 3.4 and a radius of $r=0.18a$. The photonic crystal waveguide bends are formed by two semi-infinite photonic crystals separated by a photonic crystal slab of the (10) waveguide section whose length is L.

spectrum of these three bend structures. It is clearly seen that reflectivity is in oscillatory change when frequency increases. There appears a low-reflectivity (below 1%) in the range between $\omega=0.346(2\pi c/a)$ and $\omega=0.354(2\pi c/a)$ for bend 1, in the ranges between $\omega=0.364(2\pi c/a)$ and $\omega=0.370(2\pi c/a)$ and between $\omega=0.321(2\pi c/a)$ and $\omega=0.428(2\pi c/a)$ for bend 3, and in the ranges between $\omega=0.373(2\pi c/a)$ and $\omega=0.377(2\pi c/a)$ and between $\omega=0.335(2\pi c/a)$ and $\omega=0.420(2\pi c/a)$ for bend 4. Nearly 9%, 30%, and 20% reflectivity can be found at $\omega=0.419(2\pi c/a)$ for bend 1, $\omega=0.443(2\pi c/a)$ for bend 3, and $\omega=0.436(2\pi c/a)$ for bend 4, respectively. The overall variation profiles of the reflection spectra are in good accordance with the FDTD simulation results, as one can find by comparing Fig. 6 in this paper to Fig. 4 in Ref. 9.

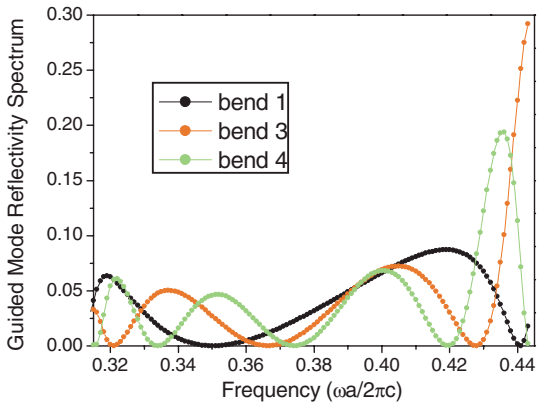

FIG. 6. (Color online) Calculated reflectivity spectrum for the waveguide bend structures shown in Figs. 5(a)–5(c).

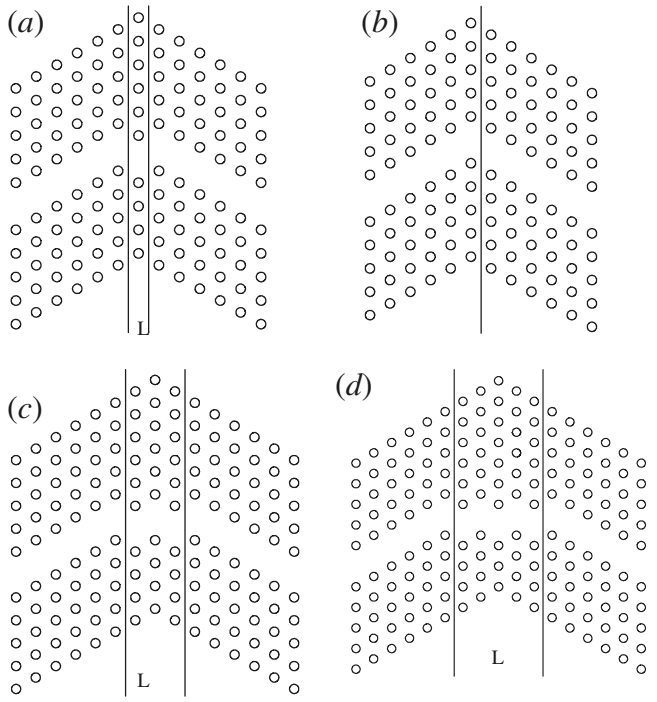

FIG. 7. Four different geometries of the 120° waveguide bend structure introduced into a triangle lattice of dielectric cylinders in air. The cylinder has a refractive index of 3.4 and a radius of $r=0.20a$. The photonic crystal waveguide bends are formed by two semi-infinite photonic crystals face to face or by two semi-infinite photonic crystals separated by a photonic crystal slab. The length of the (10) waveguide section is L.

IV. SHARP WAVEGUIDE BENDS IN TRIANGULAR LATTICE STRUCTURES

We turn to waveguide bend structures created in a 2D photonic crystal consisting of a triangular lattice of dielectric cylinders in air. Several kinds of waveguide bends are considered, and their geometric configurations are depicted in Figs. 7(a) (bend 1), 7(b) (bend 2), 7(c) (bend 3), and 7(d) (bend 4). The refractive index of the rod is 3.4 and the radius of the cylinder is $r=0.20a$. The 120° bend is formed by connecting a (11) direction straight waveguide (along the ΓK direction of the triangular lattice) and a (1-1) direction straight waveguide. The length of the (10) waveguide section is $L=0.5\sqrt{3}a$, $L=0$, $L=1.5\sqrt{3}a$, and $L=2.5\sqrt{3}a$. The band diagram of the calculated guided mode is plotted in Fig. 8. A supercell consisting of up to 11 unit cells centered at the axis of the waveguide has been adopted, which means that the primitive lattice vector of this supercell is $\vec{a}_2=(11,0)a$ and $\vec{a}_3=(\frac{1}{2},\pm\frac{\sqrt{3}}{2})a$ for the left-side and right-side waveguide ar-

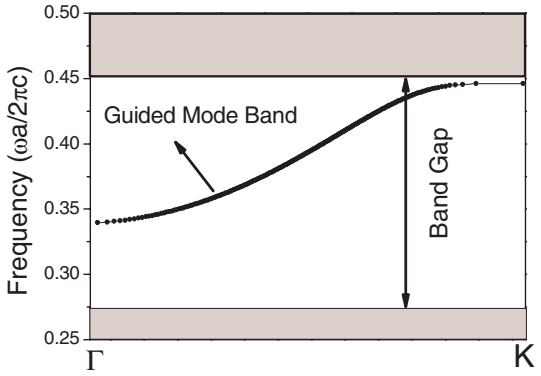

FIG. 8. (Color online) Plot of the calculated band structure of the guided modes in the waveguides shown in Fig. 8 by means of the PWTMM. The gray regions represent the lower and upper band edges of the photonic band gap for the background bulk material of photonic crystals.

rays, and the distance between adjacent waveguide axes is $11a$ in the y-axis direction. Up to 169 plane waves have been used to calculate the dispersion of the guided mode. A deliberate extrapolation technique is also used to find the exact solution of the waveguide mode under the oblique wave incidence configuration. The fundamental TM band gap lies between frequencies $0.279(2\pi c/a)$ and $0.451(2\pi c/a)$. The gray regions represent the upper and lower edges of the photonic band gap, and they are occupied by continuum photonic bands for the background bulk material. Each straight waveguide supports the single-mode operation of guided waves extending from a frequency of $\omega=0.341(2\pi c/a)$ to $\omega=0.446(2\pi c/a)$. The structure of the four waveguide bends each is well simulated by two semi-infinite PC structures connected with the sandwiched sharp waveguide bend section with thickness L. The PWTMM calculation results show that in these waveguides the summation of the transmission and reflection energy powers exactly equals the input energy power in the entire waveguide band. No artificial fluctuation due to numerical instability exists anywhere even at the waveguide cutoff frequency. Figure 9 displays the calculation results of reflection spectra for bend 1, bend 2, bend 3, and bend 4 structures. It is clearly seen that in the range between $\omega=0.341(2\pi c/a)$ and $\omega=0.358(2\pi c/a)$ for bend 1, between $\omega=0.341(2\pi c/a)$ and $\omega=0.352(2\pi c/a)$ for bend 2, between $\omega=0.341(2\pi c/a)$ and $\omega=0.362(2\pi c/a)$ for bend 3, and between $\omega=0.341(2\pi c/a)$ and $\omega=0.355(2\pi c/a)$ for bend 4, reflectivity rapidly decreases when frequency increases. However, in the range between $\omega=0.366(2\pi c/a)$ and $\omega=0.446(2\pi c/a)$ for bend 1, between $\omega=0.391(2\pi c/a)$ and $\omega=0.446(2\pi c/a)$ for bend 2, between $\omega=0.374(2\pi c/a)$ and $\omega=0.446(2\pi c/a)$ for bend 3, and between $\omega=0.352(2\pi c/a)$ and $\omega=0.446(2\pi c/a)$ for bend 4, reflectivity increases when frequency increases. There appears a relatively high-transmissivity (above 95%) and relatively low-reflectivity (below 5%) plateau in the range between $\omega=0.359(2\pi c/a)$ and $\omega=0.440(2\pi c/a)$ for the bend 1 structure, in the range between $\omega=0.353(2\pi c/a)$ and $\omega=0.426(2\pi c/a)$ for the bend 2 structure, in the range between $\omega=0.362(2\pi c/a)$ and $\omega=0.429(2\pi c/a)$ for the bend 3 structure, and in the range between $\omega=0.356(2\pi c/a)$ and $\omega=0.439(2\pi c/a)$ for the bend 4 structure.

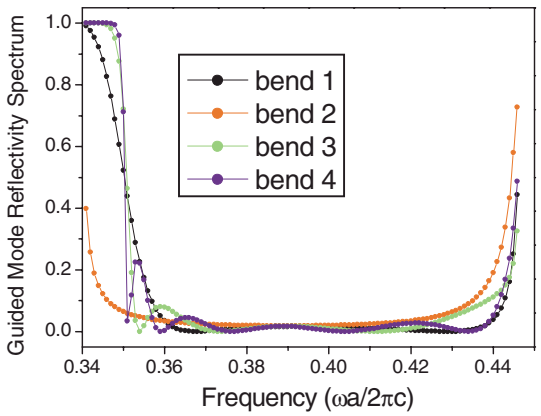

FIG. 9. (Color online) Calculated reflectivity spectrum for the waveguide bend structure shown in Figs. 7(a)–7(d).

V. CONSTRUCTION OF SUPERCELLS IN GENERAL PC WAVEGUIDE BENDS

In the above sections, we discuss how to solve the EM wave propagation problem of 2D PC waveguide bends in the framework of PWTMM. The key is the usage of a supercell technique that converts the original aperiodic structure problem into a periodic structure problem. For the 90° sharp waveguide bend in a square-lattice photonic crystal and the 120° waveguide bend in a triangular-lattice photonic crystal, one can find that the input and output waveguides both extend along a high-symmetry crystalline direction. We have selected a supercell configuration such that the lateral primitive lattice vector $\vec{a}_2$ is along a direction that bisects the angle between the input and output waveguide axes. Since $\vec{a}_2$ determines the 1D supercell grating period and the wave propagation direction, which should be perpendicular to $\vec{a}_2$, the selection of an appropriate quantity of $\vec{a}_2$ is very important. In practical simulations, for a general PC waveguide bend structure with an angle of θ as depicted in Fig. 10, the supercell size $a_2=|\vec{a}_2|$ should be as small as possible in order to reduce the computation burden. However, the coupling between adjacent supercells should be as small as possible, which requires a large supercell size. As the coupling scales with the axis-to-axis distance of adjacent waveguides, which is just $|\vec{a}_2|\sin(\theta_1)$ and $|\vec{a}_2|\sin(\theta_2)$ for the PC1 and PC2, respectively, it turns out that at $\theta_1=\theta_2=\theta/2$, the coupling is generally smallest for a given size of supercell for both the two PCs. This simple mathematics indicates that for a general PC waveguide bend with an angle θ, the optimum configuration of the supercell should be selected along the direction bisecting the angle between the input and output waveguide. In fact, such a rule has been used in studying the 2D PC waveguide bend structures in Secs. II–IV.

The above idea of constructing an appropriate supercell for a general PC waveguide can be directly extended to 3D PC waveguide bend structures. Since the waveguide now confines EM waves on two directions in the cross section

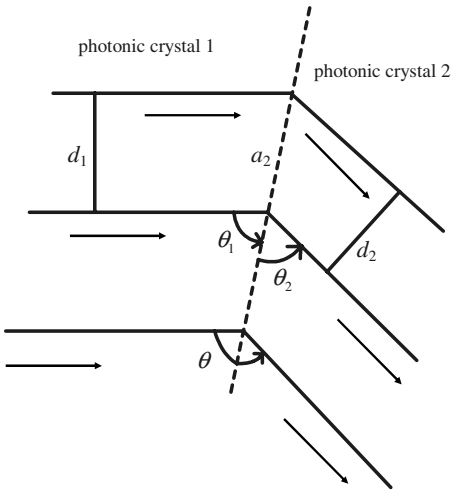

FIG. 10. Schematics showing the construction of an optimal supercell that allows for a minimum numerical computation burden by PWTMM. In the optimal configuration, the coupling between two adjacent waveguides, which is determined by the inter-waveguide distance d_1 and d_2, should be as small as possible for both input and output waveguides under a given value of the supercell size a_2. This requires that the angle satisfies $\theta_1=\theta_2=\theta/2$, where θ is the angle between the input and output waveguides.

plane, we should construct a 2D periodic waveguide array in order to describe the wave propagation problem of the 3D PC waveguide bend. In this manner, we encounter the wave scattering problem taking place at the interface between two semi-infinite 3D PC structures that model the input and output waveguides. The incident wave propagates along the stacking direction of 2D waveguide array gratings. The 3D problem can also be readily solved by PWTMM.[34–37] The construction of the supercell should follow the same principle as in the 2D PC waveguide bend situation. One primitive lattice vector of the 2D supercell $\vec{a}_2$ should be also chosen to lie within the plane (noted as M) formed by the input and output waveguides and extend along the direction bisecting the angle between the two waveguides. The other primitive lattice vector $\vec{a}_1$ can be simply set to be perpendicular to plane M. Obviously, $\vec{a}_1 \perp \vec{a}_2$, and we have a square-lattice 2D gratings to describe the 3D PC waveguide. The off-plane primitive vector $\vec{a}_3$ depends on the specific geometric structure of the considered 3D PC waveguides.

VI. CONCLUSIONS

In summary, we have developed a theoretical approach based on the PWTMM to investigate the propagation of EM waves through sharp bends of PC waveguides. In this method, artificial periodic waveguide arrays are used to model the original single waveguide. With a sufficiently large separation between adjacent waveguides, the structure does not bring any impact to the original wave propagation problem. The incorporation of this supercell technique enables us to model the original PC waveguide bend by two semi-infinite photonic crystal waveguide arrays face to face or by two semi-infinite photonic crystal waveguide arrays separated by a sandwiched slab of bend region. As a result, the original wave propagation problem is converted into the usual scattering problem of waveguide modes at the interface of two semi-infinite photonic crystal structures that can be readily solved by the PWTMM in combination with the supercell technique.

The proposed method completely removes the difficulty of separating the input, reflection, and transmission pulses as routinely encountered in the usual FDTD simulation for a waveguide bend structure of finite arm lengths. The transmission and reflection waveguide modes can be automatically extracted from the solution of the eigenmode scattering problem. The resulting transmission and reflection spectra of waveguide modes strictly satisfy the energy power conservation and are free from any numerical instability induced artificial fluctuation in the entire waveguide band. The difficulty is common in the usual FDTD simulation, particularly at the frequency close to the waveguide cutoff frequency, and can only be removed by adopting very deliberate absorbing boundary conditions. The proposed PWTMM is very numerically friendly because it only needs to calculate the transfer matrix for a single unit-cell layer and solve the corresponding eigenmodes.

We have employed the developed PWTMM to investigate several examples of waveguide bend structures created in a 2D photonic crystal made from a square or triangle lattice of dielectric cylinders in air under the TM-mode excitation. These standard structures have been investigated extensively by different methods and are also taken as examples to demonstrate the principle and power of the current PWTMM. The calculated spectra by the PWTMM are in good agreement with existing results reported in the literatures. It indicates that the PWTMM can efficiently and accurately extract the intrinsic transmission and reflection spectra of input waveguide modes in a sharp PC waveguide bend. Although in this work we only focus on the TM polarization state for 2D PC structures, the PWTMM can directly extend to handle 3D PC bend structures with any polarization states because the basic formulation has been proven to be effective and efficient for these complex structures in our previous works.[34,36] Because the domain size of the bend system used in the PWTMM has been reduced to the smallest one (single unit-cell layer) and since reliable transmission and reflection spectra information can be extracted from such small-domain computations, we expect that the method can be used to design optimal waveguide bend structures in different photonic crystal structures of arbitrary geometries.

ACKNOWLEDGMENTS

This work was supported by the State Key Development Program for Basic Research of China under Grant No. 2007CB613205 and No. 2006CB921702 and the National Natural Science Foundation of China under Grant No. 10525419.

*lizy@aphy.iphy.ac.cn

[1] S. Datta, C. T. Chan, K. M. Ho, and C. M. Soukoulis, Phys. Rev. B **48**, 14936 (1993).
[2] V. Karathanos, N. Stefanou, and A. Modinos, J. Mod. Opt. **42**, 619 (1995).
[3] F. Genereux, S. W. Leonard, H. M. van Driel, A. Birner, and U. Gosele, Phys. Rev. B **63**, 161101(R) (2001).
[4] A. A. Krokhin, P. Halevi, and J. Arriaga, Phys. Rev. B **65**, 115208 (2002).
[5] A. A. Krokhin and E. Reyes, Phys. Rev. Lett. **93**, 023904 (2004).
[6] E. Reyes, A. A. Krokhin, and J. Roberts, Phys. Rev. B **72**, 155118 (2005).
[7] J. D. Joannopoulos, R. D. Meade, and J. Winn, *Photonic Crystals* (Princeton University Press, Princeton, NJ, 1995).
[8] E. Yablonovitch, Phys. Rev. Lett. **58**, 2059 (1987).
[9] A. Mekis, J. C. Chen, I. Kurland, S. Fan, P. R. Villeneuve, and J. D. Joannopoulos, Phys. Rev. Lett. **77**, 3787 (1996).
[10] S. Y. Lin, E. Chow, V. Hietala, P. R. Villeneuve, and J. D. Joannopoulos, Science **282**, 274 (1998).
[11] S. G. Johnson, P. R. Villeneuve, S. Fan, and J. D. Joannopoulos, Phys. Rev. B **62**, 8212 (2000).
[12] A. Chutinan and S. Noda, Phys. Rev. B **62**, 4488 (2000).
[13] M. Tokushima, H. Kosaka, A. Tomita, and H. Yamada, Appl. Phys. Lett. **76**, 952 (2000).
[14] E. Chow, S. Y. Lin, S. G. Johnson, P. R. Villeneuve, J. D. Joannopoulos, J. R. Wendt, G. A. Vawter, W. Zubrzycki, H. Hou, and A. Allenman, Nature (London) **407**, 983 (2000).
[15] A. Chutinan and S. Noda, Appl. Phys. Lett. **75**, 3739 (1999).
[16] M. Bayindir, E. Ozbay, B. Temelkuran, M. M. Sigalas, C. M. Soukoulis, R. Biswas, and K. M. Ho, Phys. Rev. B **63**, 081107(R) (2001).
[17] Z. Y. Li and K. M. Ho, J. Opt. Soc. Am. B **20**, 801 (2003).
[18] R. J. Liu, Z. Y. Li, F. Zhou, and D. Z. Zhang, Opt. Express **15**, 15531 (2007).
[19] R. J. Liu, M. Ruan, Z. Y. Li, B. Y. Cheng, and D. Z. Zhang, J. Appl. Phys. **103**, 034502 (2008).
[20] K. M. Ho, C. T. Chan, and C. M. Soukoulis, Phys. Rev. Lett. **65**, 3152 (1990).
[21] Z. Y. Li, J. Wang, and B. Y. Gu, Phys. Rev. B **58**, 3721 (1998).
[22] J. B. Pendry, J. Mod. Opt. **41**, 209 (1994).
[23] L. Li, J. Opt. Soc. Am. A **13**, 1024 (1996).
[24] A. Taflove and S. C. Hagness, *Computational Electrodynamics: The Finite-Difference Time-Domain Method* (Artech House, Boston, 1995).
[25] A. Mekis, S. Fan, and J. D. Joannopoulos, IEEE Microw. Guid. Wave Lett. **9**, 502 (1999).
[26] M. Koshiba, Y. Tsuji, and S. Sasaki, IEEE Microw. Wirel. Compon. Lett. **11**, 152 (2001).
[27] Z. Y. Li and K. M. Ho, Phys. Rev. B **68**, 045201 (2003).
[28] K. Busch, S. F. Mingaleev, A. Garcia-Martin, M. Schillinger, and D. Hermann, J. Phys.: Condens. Matter **15**, R1233 (2003).
[29] Y. Jiao, S. H. Fan, and D. A. B. Miller, Opt. Lett. **30**, 141 (2005).
[30] E. Moreno, D. Erni, and C. Hafner, Phys. Rev. E **66**, 036618 (2002).
[31] J. Smajic, C. Hafner, and D. Erni, Opt. Express **11**, 1378 (2003).
[32] W. J. Kim and J. D. Obrien, J. Opt. Soc. Am. B **21**, 289 (2004).
[33] J. S. Jensen and O. Sigmund, Appl. Phys. Lett. **84**, 2022 (2004).
[34] Z. Y. Li and L. L. Lin, Phys. Rev. E **67**, 046607 (2003).
[35] L. L. Lin, Z. Y. Li, and K. M. Ho, J. Appl. Phys. **94**, 811 (2003).
[36] Z. Y. Li and K. M. Ho, Phys. Rev. B **68**, 245117 (2003).
[37] Z. Y. Li and K. M. Ho, Phys. Rev. B **68**, 155101 (2003).
[38] Z. Y. Li, L. L. Lin, and K. M. Ho, Appl. Phys. Lett. **84**, 4699 (2004).
[39] M. Che, Z. Y. Li, and R. J. Liu, Phys. Rev. A **76**, 023809 (2007).
[40] A. Figotin and I. Vitebskiy, Phys. Rev. E **68**, 036609 (2003).
[41] Y. C. Hsue and T. J. Yang, Phys. Rev. E **70**, 016706 (2004).
[42] E. Istrate and E. H. Sargent, Rev. Mod. Phys. **78**, 455 (2006).